PERSPECTIVE

Quantifying an acceptable open-circuit corrosion current for aluminum–air batteries†

Brandon J. Hopkins [ID] *[a] and Debra R. Rolison [ID] [b]

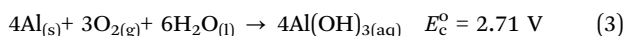Primary aluminum–air batteries achieve impressive specific-energy values but suffer from poor shelf life due to corrosion of the aluminum anode in aqueous electrolytes. To solve this problem, researchers investigate numerous corrosion-mitigation strategies. Few rigorously compare the performance of these strategies, and most fail to define a technologically acceptable open-circuit corrosion current. To compete with commercialized zinc–air batteries, aluminum–air batteries need open-circuit corrosion currents less than 0.01 mA cm_{geo}^{-2}, which we derive by performing a sensitivity analysis on a corrosion model reported here. By conducting a meta-analysis using reported aluminum–air cells, we find that certain ionic-liquid electrolytes and oil-displacement systems enable corrosion currents that meet this metric. In contrast, values for commonly reported aluminum–air batteries using alkaline electrolytes are orders of magnitude too high. Once the aluminum–air community focuses on advancing appropriate corrosion-mitigation strategies, laboratory findings may become commercially relevant.

Introduction

Primary, *i.e.*, not electrically rechargeable, aluminum–air (Al–air) batteries are projected to achieve high practical system-level specific energies near 1000 W h kg_{sys}^{-1} depending on their design, but most suffer from severe Al-anode corrosion in aqueous electrolytes that dramatically reduces shelf life.[1] During Al–air discharge, oxygen is reduced, and Al is simultaneously oxidized (eqn (1)–(3); potentials are measured with respect to the standard hydrogen electrode, SHE, for half reactions).[2]

$$O_{2(g)} + 2H_2O_{(l)} + 4e^- \rightarrow 4OH_{(aq)}^- \quad E_a^o = 0.40 \text{ V } vs. \text{ SHE} \quad (1)$$

$$Al_{(s)} + 3OH_{(aq)}^- \rightarrow Al(OH)_{3(aq)} + 3e^- \quad E_b^o = 2.31 \text{ V } vs. \text{ SHE} \quad (2)$$

$$4Al_{(s)} + 3O_{2(g)} + 6H_2O_{(l)} \rightarrow 4Al(OH)_{3(aq)} \quad E_c^o = 2.71 \text{ V} \quad (3)$$

However, when an Al–air battery is idle or in open-circuit conditions, a parasitic corrosion reaction occurs at the Al anode in aqueous electrolytes, resulting in unwanted hydrogen evolution and Al oxidation (eqn (5); derived using eqn (2) and (4)).[2]

$$2H_2O_{(l)} + 2e^- \rightarrow H_{2(g)} + 2OH_{(aq)}^- \quad E_d^o = -0.83 \text{ V } vs. \text{ SHE} \quad (4)$$

$$2Al_{(s)} + 6H_2O_{(l)} \rightarrow 2Al(OH)_{3(s)} + 3H_{2(g)} \quad E_e^o = 1.48\text{V} \quad (5)$$

Aluminum-anode corrosion can also occur during discharge, but open-circuit corrosion dictates shelf life, which is the focus of this perspective. Since Zaromb published the first known report on Al–air batteries in 1962, many continue to search for corrosion mitigation strategies for Al–air batteries.[3] Once researchers overcome this self-discharge problem, primary Al–air batteries will become low-cost, energy-dense forms of electrochemical energy storage with applications in robotics,[4] electric aviation,[5] wearable power,[6] off-grid power,[7] and vehicle range extension.[8]

Methods to suppress open-circuit Al anode corrosion include anode alloying,[9–14] electrolyte additives,[15–22] saline electrolytes,[23,24] ionic-liquid electrolytes,[25,26] dual electrolytes,[27] gel electrolytes,[28] anode films,[28] cold temperatures,[29] anode grain sizes,[24,30] anode crystal orientations,[31] and oil displacement systems.[32] Despite this growing list, few studies rigorously compare the performance of these strategies.[33–38] In addition, the Al–air community has yet to clarify a technologically acceptable open-circuit corrosion rate, measured as a corrosion current with units of mA cm_{geo}^{-2} (with respect to the geometric area of the Al anode).

Here, we address these issues by first reporting an Al-anode corrosion model, which shows that Al–air batteries need open-circuit corrosion currents less than 0.01 mA cm_{geo}^{-2} to compete with commercialized zinc–air (Zn–air) batteries. In contrast, a past report suggests that a corrosion current of 0.1 mA cm_{geo}^{-2} may be technologically relevant but provides minimal analysis for this conclusion.[34] Second, we compare corrosion mitigation

[a] *National Research Council Postdoctoral Associate, Surface Chemistry Branch, U.S. Naval Research Laboratory, Code 6170, Washington, DC 20375, USA. E-mail: brandon.hopkins.ctr@nrl.navy.mil*

[b] *Surface Chemistry Branch, U.S. Naval Research Laboratory, Code 6170, Washington, DC 20375, USA*

strategies by plotting their open-circuit corrosion currents *versus* respective specific energies with respect to Al-anode mass and find that some ionic-liquid electrolytes and oil-displacement systems meet this corrosion-current metric. We show that the open-circuit corrosion currents of commonly reported Al–air batteries that use alkaline electrolytes are orders of magnitude too high even if they use corrosion-mitigation strategies involving anode alloying, electrolyte additives, anode grain sizes, or anode crystal orientations.

Deriving an acceptable open-circuit corrosion current

The self-discharge rate of Al–air batteries must approach that of Zn–air batteries to advance commercially, requiring an Al-anode corrosion current less than 0.01 mA cm_{geo}^{-2}. Currently primary Zn–air batteries, used in hearing aids, are the only widely available metal–air battery and have self-discharge rates of 2% y^{-1}.[39,40] Using this value, we calculate a practical upper-bound corrosion current based on a sensitivity analysis of a corroding Al-anode plate reported here. With the outlined independent variables (Table 1), we derive dependent variables (Table 2) to calculate open-circuit corrosion current as a function of self-discharge rate.

The derived corrosion current is based on Al-anode-plate mass and geometric surface area. We assume that the Al anode is square shaped. The quotient of Al-anode mass divided by the geometric surface area of the plate (M_{Al}/A_{Al}) alters open-circuit corrosion current (I_{corr}). Once corrosion commences, this quotient changes with time. Some corrosion-current measurements take this effect into account by measuring open-circuit corrosion current as a function of time or by reporting an approximate steady-state value.[41] We note that measurements of open-circuit corrosion current depend on multiple variables such as temperature, total electrolyte volume, whether or not the electrolyte is flowing or static, and the amount of Al that is already dissolved in the electrolyte. By plotting corrosion current as a function of Al-anode length and thickness while requiring a self-discharge rate of 2% y^{-1}, we show that Al-anode geometry substantially impacts the required open-circuit corrosion current. The larger and thicker the Al anode, the greater the acceptable corrosion current (Fig. 1).

Even for exceptionally large, thick Al anodes (30 cm in length and 1 cm in thickness), the corrosion current must be less than 0.01 mA cm_{geo}^{-2}. We note that thick Al anodes are acceptable because discharge reactions only occur at the surface of the Al anode. No ion transport happens within the Al-anode volume. In addition, one could argue that some Al–air cells such as those in a reserve battery, which stores electrolyte separate from its Al anodes until first use, do not need to achieve such low self-discharge rates. While true, reserve batteries are generally only used for niche military applications.

We note that potential applications, which have yet to be commercialized, may allow for a corrosion current greater than 0.01 mA cm_{geo}^{-2}. For example, if a primary Al–air battery acted as a replacement for a gasoline-based range extender for an electric vehicle, a self-discharge rate of 50% y^{-1} may be acceptable because the shelf life of gasoline varies between 3 and 6 months depending on how the gasoline is stored. Using the same analysis from which we derive the 0.01 mA cm_{geo}^{-2} benchmark, we calculate an acceptable corrosion current of 0.25 mA cm_{geo}^{-2} for a range-extender scenario.

Comparing corrosion-mitigation strategies

By plotting the open-circuit corrosion current *versus* respective specific energy of reported corrosion-mitigation strategies,[9–32] we find that certain ionic-liquid electrolytes[25] and oil-displacement systems[32] can meet the open-circuit corrosion current metric of 0.01 mA cm_{geo}^{-2}, but Al–air cells using ionic-liquid electrolytes sacrifice specific energy (Fig. 2; Table S1, ESI†). For vehicle-range extender applications, saline electrolytes[23,24] and anode films with gel electrolyte[28] meet the less strict 0.25 mA cm_{geo}^{-2} metric. Ideal corrosion-mitigation strategies achieve low open-circuit corrosion current and high specific energy (bottom-right corner of Fig. 2). To the best of our ability, Fig. 2, which includes 26 Al–air cells, is nearly comprehensive based on available data. Using the search term "aluminum–air battery" on Web of Science, we find that the majority of the 217 listed Al–air reports fail to include full-cell testing and measurements of both open-circuit corrosion current and specific energy with respect to Al-anode mass.

To date, Al–air batteries that use alkaline electrolytes fail to achieve open-circuit corrosion currents below 1 mA cm_{geo}^{-2} even if they use strategies involving anode alloying, electrolyte additives, anode grain sizes, or anode crystal orientations (Fig. 2). Assuming a best case scenario where the Al anode is large (30 cm in length and 1 cm in thickness), a corrosion current of 1 mA cm_{geo}^{-2} translates to a self-discharge rate of 230% y^{-1} or 20% per month. Using baseline values (Table 1) for

Table 1 Independent variables of the Al-anode corrosion model

Variable	Description	Units	Range	Baseline
d_{Al}	Density of Al	g cm^{-3}	Fixed	2.7
m_{Al}	Molar mass of Al	g mol^{-1}	Fixed	26.98
n	Moles of electrons per mole of Al	Unitless	Fixed	3
F	Coulombs per mole of electrons	C mol^{-1}	Fixed	96 485
S_{Al}	Self-discharge rate	% y^{-1}	Fixed	2
$C_{s/y}$	Number of seconds per year	s y^{-1}	Fixed	3.154×10^7
L_{Al}	Side length of Al plate	cm	1–30	10
T_{Al}	Thickness Al plate	cm	0.10–1.00	0.50

Table 2 Dependent variables of the Al-anode corrosion model

Variable	Description	Units	Derivation
M_{Al}	Mass of Al plate	g	$M_{Al} = L_{Al}^2 \times T_{Al} \times d_{Al}$
A_{Al}	Geometric surface area of Al plate	cm_{geo}^2	$A_{Al} = 2 \times L_{Al}^2 + 4 \times L_{Al} \times T_{Al}$
I_{corr}	Open-circuit corrosion current	$A\ cm_{geo}^{-2}$	$I_{corr} = \dfrac{M_{Al} \times F \times n \times \left(\dfrac{S_{Al}}{100}\right)}{A_{Al} \times C_{s/y} \times m_{Al}}$

Fig. 1 Open-circuit corrosion current *versus* Al-anode length and thickness while requiring a self-discharge rate of 2% y^{-1}. We calculate open-circuit corrosion current using the equation in Table 2.

an Al anode (10 cm in length and 0.5 cm in thickness), a corrosion current of 1 mA cm$_{geo}^{-2}$ yields a self-discharge rate of 480% y^{-1} or 40% per month. Either of these scenarios is unacceptable for most applications due to poor shelf life. One can perform such calculations by solving for self-discharge rate (S_{Al}) in the equation for open-circuit corrosion current (Table 2).

We also observe a general trend within and across corrosion-mitigation strategies: the lower the open-circuit corrosion current, the lower the specific energy. For example, Al–air cells using alkaline electrolytes achieve high specific energy but also high, undesirable corrosion. While alkaline electrolytes are notoriously corrosive, they provide elevated discharge voltages at aggressive current densities due to their (1) high ionic conductivity, (2) high solubility of Al and consequently effective Al oxidation, and (3) high efficiency in catalyzing oxygen reduction at the air cathode. Specifically, an alkaline-electrolyte Al–air cell can discharge at 1.5 V under 20 mA cm$_{geo}^{-2}$ with an open-circuit corrosion current near 3 mA cm$_{geo}^{-2}$.[15] In contrast, Al–air cells using ionic-liquid electrolytes enable low corrosion but also low, undesirable specific energy. Ionic-liquid electrolytes enable low corrosion currents because of their low water content, and without water, Al-anode corrosion cannot occur (eqn (5)). While ionic-liquid electrolytes induce minimal corrosion, they

provide diminished discharge voltages at feeble current densities due to their (1) low ionic conductivity, (2) low solubility of Al and consequently ineffective Al oxidation, and (3) low efficiency in catalyzing oxygen reduction at the air cathode. For example, an Al–air cell with an ionic-liquid electrolyte discharges at 0.7 V under 0.1 mA cm$_{geo}^{-2}$ with an open-circuit corrosion current near 0.003 mA cm$_{geo}^{-2}$.[25] Saline electrolytes and anode films combined with gel electrolytes allow for moderate performance that falls between the extremes of ionic-liquid electrolytes and alkaline electrolytes. Both saline electrolytes and anode films with gel electrolytes achieve (1) moderate ionic conductivity, (2) moderate solubility of Al and consequently moderately effective Al oxidation, and (3) moderate efficiency in catalyzing oxygen reduction at the air cathode.

Aluminum–air cells using oil displacement systems, however, largely decouple open-circuit corrosion current from specific energy. They achieve the lowest corrosion current in the dataset (Fig. 2) along with a high specific energy because they use alkaline electrolyte during discharge but then displace this electrolyte with oil when the battery is not in use.[32] Some corrosion continues even after oil displacement because a small portion of electrolyte dissolves in the displacing oil, yielding a low open-circuit corrosion current. Specifically, one Al–air cell using an oil displacement system can discharge near 1.3 V under 150 mA cm$_{geo}^{-2}$ with an open-circuit corrosion current of 0.0006 mA cm$_{geo}^{-2}$.[32] But this corrosion-mitigation strategy reduces projections for system-level specific energy from 1300 W h kg$_{sys}^{-1}$ for a flowing electrolyte Al–air system to 900 W h kg$_{sys}^{-1}$ because of the need for added oil and other auxiliary components. We note that these system-level specific energy projections assume that water for the Al–air battery is refilled four times to allow for full discharge. However, even a reduced specific energy of 900 W h kg$_{sys}^{-1}$ is high in comparison to electrically rechargeable lithium–air or zinc–air batteries that are projected to reach values of 450 W h kg$_{sys}^{-1}$.[42]

Some authors that report promising corrosion-mitigation strategies unfortunately fail to explicitly measure open-circuit corrosion current. For example, Zhang *et al.*[43] demonstrate an Al–air cell with a gel electrolyte that can delaminate from the Al anode during open-circuit conditions. While they show that separating the gel electrolyte from the Al anode during pauses in discharge increases battery capacity, they fail to explicitly report an open-circuit corrosion current. Corrosion may occur after a user removes the gel electrolyte from the Al anode because some electrolyte remains on the Al-anode surface. Another example of a corrosion-mitigation strategy that researchers have yet to fully characterize involves draining
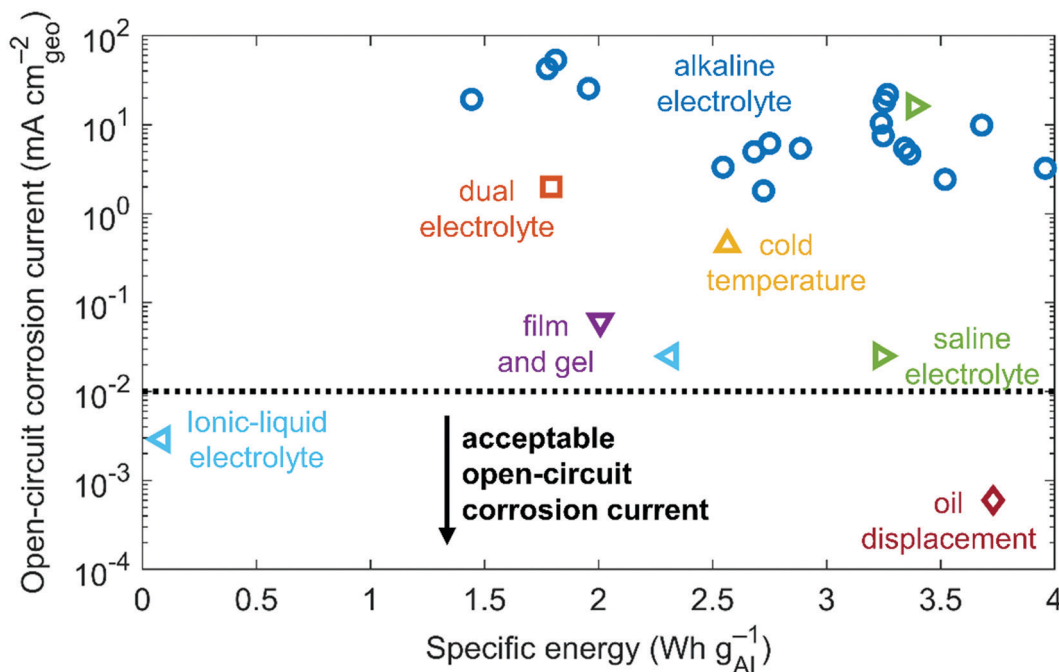
Fig. 2 Open-circuit corrosion currents *versus* respective specific energies for reported corrosion-mitigation strategies.[9–32] We group anode alloying, electrolyte additives, anode grain sizes, and anode crystal orientations into one category characterized by the use of alkaline electrolyte. Methods yielding open-circuit corrosion currents below 0.01 mA cm$_{geo}^{-2}$ are acceptable. See also Table S1 (ESI†).

liquid electrolyte from Al–air cells.[32,44,45] Reports generally conclude that electrolyte sticks to the internal surfaces of cells, which induces unacceptably high levels of corrosion. But to our knowledge, researchers have yet to quantify the open-circuit corrosion current achieved using this strategy. Modifications to cell design could enable better draining and consequently less open-circuit corrosion.

Discussion

If the open-circuit corrosion current of an Al anode in safe, inexpensive, and highly conductive electrolyte can be decreased, Al–air batteries will displace commercialized primary Zn–air batteries. Aluminum is more than 1000 times more abundant than Zn and is currently 28% less expensive.[46] Aluminum has a theoretical gravimetric capacity of 2980 mA h g$_{Al}^{-1}$ while the value for Zn is 820 mA h g$_{Zn}^{-1}$.[42] This difference arises from the fact that Al has a lower density than Zn and because the Al redox reaction, shown in eqn (2) uses three electrons, while the equivalent reaction in Zn–air batteries uses only two electrons. In addition, the practical open-circuit voltage of an Al–air cell approaches 1.8 V while that for Zn–air approaches 1.5 V.[32,46]

Based on our meta-analysis, we make the following recommendations for future research.

(1) Certain ionic-liquid electrolytes enable acceptable corrosion current but achieve poor specific energy. Because ionic-liquid electrolytes are still relatively new in the field of Al–air batteries in comparison to alkaline electrolytes, this class of electrolyte warrants more research. But we do not see a clear path to

overcome the tradeoffs associated with ionic-liquid electrolytes by themselves at this time.

(2) One strategy to enable acceptable corrosion with a high specific energy involves oil displacement systems. With few publications exploring this concept or similar concepts to date, we encourage additional research related to the displacement of electrolyte during open-circuit conditions.

(3) Some saline electrolytes are the next best option for high specific energy and low open-circuit corrosion. Using Fig. 2, we see saline electrolytes as a potentially promising and generally overlooked research avenue for Al–air batteries.

(4) Unfortunately, most reported Al–air batteries that rely on alloys or electrolyte additives with conventional alkaline electrolytes are far from approaching acceptable corrosion currents below 0.01 mA cm$_{geo}^{-2}$. Based on their poor performance over decades of research, we struggle to see conventional alkaline electrolytes playing a substantial role in future Al–air batteries. Even for potential applications that allow for high self-discharge rates such as electrochemical fuel for vehicle range extenders, a user would need to initiate discharge upon fueling with fresh Al anodes. For reserve batteries that deliver uninterrupted discharge or discharge with short pauses, alkaline electrolytes are still a top choice.

(5) We see a promising future in combining multiple corrosion mitigation strategies to boost performance. For example, the standout saline-electrolyte performer[24] shown in Fig. 2 uses an alloyed Al anode, saline electrolyte, and a modified Al-anode microstructure, which was tuned by rolling cast ingots of Al alloy. By combining these three strategies, the authors achieve better performance than they would have if they had only used one strategy.

Author contributions

B. J. H. contributed in the roles of conceptualization, data curation, formal analysis, visualization, writing – original draft, and writing – review & editing. D. R. R. contributed in the roles of conceptualization, funding acquisition, and writing – review & editing.

Conflicts of interest

B. J. H. is a named inventor on provisional patents related to aluminum–air batteries: US patent no. 2019/0123407 A1 and 2019/0326603 A1. D. R. R. is a named inventor on patents related to zinc electrodes: US Patents no. 9802254, 10008711, 10720635, 10763500, and 10804535, EU Patent no. 2926395, and China Patent no. 104813521.

Acknowledgements

References

1 S. Yang and H. Knickle, *J. Power Sources*, 2002, **112**, 162–173.

2 S. G. Bratsch, *J. Phys. Chem. Ref. Data*, 1989, **18**, 1–21.

3 S. Zaromb, *J. Electrochem. Soc.*, 1962, **109**, 1125–1130.

4 M. Wang, U. Joshi and J. H. Pikul, *ACS Energy Lett.*, 2020, **5**, 758–765.

5 B. J. Hopkins, J. W. Long, D. R. Rolison and J. F. Parker, *Joule*, 2020, **4**, 2237–2243.

6 Y. Ma, A. Sumboja, W. Zang, S. Yin, S. Wang, S. J. Pennycook, Z. Kou, Z. Liu, X. Li and J. Wang, *ACS Appl. Mater. Interfaces*, 2018, **11**, 1988–1995.

7 S. C. Mok, IEEE Global Humanitarian Technological Conference, 10.1109/GHTC.2011.11 (accessed 1 December 2020).

8 M. Gebrehiwot and A. Van den Bossche, *Int. J. Automot. Technol.*, 2015, **16**, 707–713.

9 J. Ren, J. Ma, J. Zhang, C. Fu and B. Sun, *J. Alloys Compd.*, 2019, **808**, 151708.

10 H. Wen, Z. Liu, J. Qiao, R. Chen, R. Zhao, J. Wu, G. Qiao and J. Yang, *Int. J. Energy Res.*, 2020, **44**, 7468–7579.

11 L. Fan, H. Lu, J. Leng, Z. Sun and C. Chen, *J. Electrochem. Soc.*, 2016, **163**, A8–A12.

12 S. Zhou, C. Tian, S. Alzoabi, Y. Xu, Z. Jiao, K. Luo, B. Peng, C. Zhang, N. Santos and Y. Cao, *J. Mater. Sci.*, 2020, **55**, 11477–11488.

13 I.-J. Park, S.-R. Choi and J.-G. Kim, *J. Power Sources*, 2017, **357**, 47–55.

14 Y.-J. Cho, I.-J. Park, H.-J. Lee and J.-G. Kim, *J. Power Sources*, 2015, **277**, 370–378.

15 M. A. Deyab, *Electrochim. Acta*, 2017, **244**, 178–183.

16 J. Ma, Y. Zhang, C. Qin, F. Ren and G. Wang, *Int. J. Hydrogen Energy*, 2020, **45**, 13025–13034.

17 S. Wu, Q. Zhang, D. Sun, J. Luan, H. Shi, S. Hu, Y. Tang and H. Wang, *Chem. Eng. J.*, 2020, **383**, 123162.

18 M. A. Deyab, *J. Power Sources*, 2019, **412**, 520–526.

19 Y. Liu, H. Zhang, Y. Liu, J. Li and W. Li, *J. Power Sources*, 2019, **434**, 226723.

20 S. Wu, S. Hu, Q. Zhang, D. Sun, P. Wu, Y. Tang and H. Wang, *Energy Storage Mater.*, 2020, **31**, 310–317.

21 C. Zhu, H. Yang, A. Wu, D. Zhang, L. Gao and T. Lin, *J. Power Sources*, 2019, **432**, 55–64.

22 H. Jiang, S. Yu, W. Li, Y. Yang, L. Yang and Z. Zhang, *J. Power Sources*, 2020, **448**, 227460.

23 Z. Wu, H. Zhang, K. Qin, J. Zou, K. Qin, C. Ban, J. Cui and H. Nagaumi, *J. Mater. Sci.*, 2020, **55**, 11545–11560.

24 X. Yin, K. Yu, T. Zhang, H. Fang, H. Dai, H.-Q. Xiong and Y.-L. Dai, *Int. J. Electrochem. Sci.*, 2017, **12**, 4150–4163.

25 R. Revel, T. Audichon and S. Gonzalez, *J. Power Sources*, 2014, **272**, 415–421.

26 D. Gelman, B. Shvartsev and Y. Ein-Eli, *J. Mater. Chem. A*, 2014, **2**, 20237–20242.

27 P. Teabnamang, W. Kao-ian, M. T. Nguyen, T. Yonezawa, R. Cheachareon and S. Kheawhom, *Energies*, 2020, **13**, 2275.

28 Y. Zuo, Y. Yu, H. Liu, Z. Gu, Q. Cao and C. Zuo, *Batteries*, 2020, **6**, 19.

29 Y. Zuo, Y. Yu, C. Zuo, C. Ning, H. Liu, Z. Gu, Q. Cao and C. Shen, *Energies*, 2019, **12**, 612.

30 Y. Han, J. Ren, C. Fu, M. Jiang, S. Lu, J. Zhang and B. Sun, *J. Electrochem. Soc.*, 2020, **167**, 040514.

31 L. Fan, H. Lu, J. Leng, Z. Sun and C. Chen, *J. Power Sources*, 2015, **299**, 66–69.

32 B. J. Hopkins, Y. Shao-Horn and D. P. Hart, *Science*, 2018, **362**, 658–661.

33 Q. Li and N. J. Bjerrum, *J. Power Sources*, 2020, **110**, 1–10.

34 D. R. Egan, C. Ponce de Léon, R. J. K. Wood, R. L. Jones, K. R. Stokes and F. C. Walsh, *J. Power Sources*, 2013, **236**, 293–310.

35 M. Mokhtar, M. Z. M. Talib, E. H. Majlan, S. M. Tasirin, W. M. F. W. Ramli, W. R. W. Daud and J. Sahari, *J. Ind. Eng. Chem.*, 2015, **32**, 1–20.

36 Y. Liu, Q. Sun, W. Li, K. R. Adair, J. Li and X. Sun, *Green Energy Environ.*, 2017, **2**, 246–277.

37 J. Ryu, M. Park and J. Cho, *Adv. Mater.*, 2019, **31**, 1804784.

38 P. Goel, D. Dobhal and R. C. Sharma, *J. Energy Storage*, 2020, **28**, 101287.

39 Duracell, Technical Library, https://www.duracell.com/, accessed 1 December 2020.

40 B. J. Hopkins, M. B. Sassin, C. N. Chervin, P. A. DeSario, J. F. Parker and D. R. Rolison, *Energy Storage Mater.*, 2020, **27**, 370–376.

41 D. Gelman, I. Lasman, S. Elfimchev, D. Starosvetsky and Y. Ein-Eli, *J. Power Sources*, 2015, **285**, 100–108.

42 B. J. Hopkins, C. N. Chervin, J. W. Long, D. R. Rolison and J. F. Parker, *ACS Energy Lett.*, 2020, **5**, 3405–3408.

43 Z. Zhang, C. Zuo, Z. Liu, Y. Yu, Y. Zuo and Y. Song, *J. Power Sources*, 2014, **251**, 470–475.

44 T. A. Dougherty, A. P. Karpinski, S. P. Lapp, R. N. Kallok and S. V. Natale, Proceedings of INTELEC 95. 17th International Telecommunications Energy Conference, https://doi.org/10.1109/INTLEC.1995.499054, accessed 1 December 2020.

45 D. Tzidon and I. Yakupov, *US Pat.*, US 9627726 B2, 2017.

46 B. J. Hopkins, C. N. Chervin, M. B. Sassin, J. W. Long, D. R. Rolison and J. F. Parker, *Sustainable Energy Fuels*, 2020, **4**, 3363–3369.